Available online at www.sciencedirect.com
SCIENCE DIRECT®
Energy and Buildings xxx (2005) xxx–xxx
ENERGY and BUILDINGS
www.elsevier.com/locate/enbuild

Prediction of building's temperature using neural networks models

A.E. Ruano [a,*], E.M. Crispim [a], E.Z.E. Conceição [b], M.M.J.R. Lúcio [c]

[a] *Centre for Intelligent Systems, Faculty of Sciences and Technology, University of Algarve, Campus de Gambelas, 8005-139 Faro, Portugal*
[b] *Faculty of Marine and Environmental Sciences, University of Algarve, Campus de Gambelas, 8005-139 Faro, Portugal*
[c] *Direcção Regional de Educação do Algarve, Sítio das Figuras, EN 125, 8000-761 Faro, Portugal*

Received 21 March 2005; received in revised form 29 August 2005; accepted 2 September 2005

Abstract

The use of artificial neural networks in various applications related with energy management in buildings has been increasing significantly over the recent years. In this paper the design of inside air temperature predictive neural network models, to be used for predictive control of air-conditioned systems, is discussed.

The use of multi-objective genetic algorithms for designing off-line radial basis function neural network models is detailed. The performance of these data-driven models is compared, favourably, with a multi-node physically based model. Climate and environmental data from a secondary school located in the south of Portugal, collected by a remote data acquisition system, are used to generate the models. By using a sliding window adaptive methodology, the good results obtained off-line are extended throughout the whole year. The use of long-range predictive models for air-conditioning systems control is demonstrated, in simulations, achieving a good temperature regulation with important energy savings.

Keywords: Temperature prediction; Neural networks; Multi-objective genetic algorithm; Radial basis function networks

1. Introduction

The use of artificial neural networks in various applications related with energy management in buildings has been increasing significantly over the recent years. Artificial neural networks (ANNs) have been applied, for instance, in renewable energy systems (see for instance the review in Ref. [1] and the references within Ref. [2]), in heating, ventilation and air conditioning (HVAC) control methodologies [3–9], and in forecasting energy consumption [10].

Of special interest to this area is the use of ANNs for forecasting the room(s) air temperature as a function of both forecasted weather parameters (mainly solar radiation and air temperature) and actuator (heating, ventilating, cooling) state or manipulated variables, and the subsequent use of these mid/long-range prediction models for a more efficient temperature control, both in terms of regulation and energy consumption.

Estimating the inside air temperature inside buildings is a complicated task, which can be tackled with two different classes of models: physical or white-box models, and data-driven or black-box models. Both can be viewed as a non-linear dynamical system and use as inputs weather parameters and actuators manipulated variables, and as output the predicted room temperature.

Physical models are based on energy and mass balance integral–differential equations. This physical model philosophy permits to study and evaluate the thermal efficiency of building constructions. The building simulation is important not only in the before-project, but also in the after-project phase, in the evaluation and improvement of the thermal solution. Nevertheless, in this kind of model is important, before the final simulation phase, to validate the numerical model using, normally, the experimental results obtained in real situation. This physical model can be used in Winter and Summer conditions studies being considered the occupation cycle, external and internal windows shading devices, submersed ducts, natural and forced ventilation, heating and air-conditioning systems, collectors systems used to heat the water, radiant panels in the floor, wall or ceiling, among others. Once the parameters of the model have been determined, they remain fixed afterwards. The development time of such a type of model for a medium-size building is usually a very time-consuming task, and a complete simulation in a modern Personal Computer (PC) usually takes days of computational

* Corresponding author.
E-mail address: aruano@ualg.pt (A.E. Ruano).

0378-7788/$ – see front matter © 2005 Elsevier B.V. All rights reserved.
doi:10.1016/j.enbuild.2005.09.007

time. This physical model calculates not only the temperature of the air inside the different compartments and ducts system, the several windows glasses, the different interior bodies (furniture, curtains, ...) located inside spaces and the several slices of the building main bodies (doors, walls, ground, roofs, ceilings, ...) and ducts systems, but also the water vapour mass inside spaces, ducts systems and in the interior surfaces and the mass of contaminants inside spaces and ducts system. It also calculates the real distribution of incident solar radiation in the internal and external surfaces, the view factors between different interior surfaces in each space, the radiative heat exchange between internal surfaces, the radiative heat exchange between the building external surfaces and the surrounding bodies, the glasses radiative coefficients, the heat and mass transfer coefficients by convection between the surfaces and the air, the air relative humidity inside different compartments, the mass transfer between different spaces and between several spaces and the external environment and the global thermal comfort level inside each space. Physical models can be employed to provide forecasts of these inside climate variables even before the actual building is built.

Black-box models, such as neural networks, depend completely on experimental data and therefore can only be developed after the actual building is built and measurements are available. Typically, for each room in a building and for each variable of interest a separate model must be designed. Due to their universal approximation properties [11–13] neural networks can approximate well the complex relationship between the system inputs (in this case the weather parameters and actuators manipulated variables) and the inside air temperature. In this class of models the model parameters are the number of neurons and the values of interconnection weights, which do not have any physical meaning. As the system to be modelled is dynamic, if external dynamic neural models are employed, the number of lags and the determination of which lags to be employed for the model inputs is also a task to be solved during model development. Although model development time depends on the designer expertize and on the tools available, the construction time for this kind of models is typically much less than for physical models. Once a model is developed, a complete simulation takes a few minutes (in contrast with a few days for physical models), which enables its use for real-time control of HVAC systems. Additionally, in contrast with physical models, neural networks can be made adaptive, by changing their parameters as a function of the actual performance that the models exhibit.

The role of these two different types of models is therefore complementary, and not competing. While physical models can be used in the phase of the project of buildings, and to assess the consequences of possible buildings modifications, data-driven models, such as neural networks, should be used for the on-line control of HVAC systems.

The main focus of this paper is the design of neural network models for temperature prediction inside buildings. This involves, in a first stage, finding the best structure of the model—the number of neurons and the number and determination of input lags, and the estimation of the network parameters. The model structure will be determined using a multi-objective genetic algorithm (MOGA), while parameter estimation will be performed by the application of the Levenberg–Marquardt algorithm, exploiting the linear–non-linear separability of the model parameters. In a second stage, the off-line determined neural model will be adapted on-line, through the use of a sliding-window based algorithm. The performance of the neural model will be compared with a physical model using as a test case data collected from a public secondary scholar building situated in the south of Portugal. A preliminary example of the use of predictive neural models for the control of an air-conditioned system will be shown, illustrating both the better regulation and the energy savings obtained.

The layout of the paper is as follows: Section 2 describes the experimental setup. Section 3 explains the physical model developed and shows results obtained with this model. Section 4 introduces the neural networks employed, radial basis functions, and discusses the parameter estimation algorithm employed. Section 5 addresses the use of multi-objective genetic algorithms for topology determination and input selection and illustrates the results obtained in the off-line training phase. A comparison between neural models and physical models is also presented in this section. Adaptive models are addressed in Section 7. The use of neural models for the control of an air-conditioned system is discussed in Section 8. The paper ends with conclusions and a description of future work.

2. Experimental setup

The data set used came from a remote data acquisition system implemented in a secondary school building (Escola EB2/3 of Estoí) located in the south region of Portugal, the Algarve, where in 90% of the year the sky is clear.

The purpose of this data acquisition system is to collect environmental information from inside and outside the secondary school. The outdoor equipment consists of a meteorological station composed of an Environdata data-logger, and air temperature, air humidity, solar radiation, wind speed and direction sensors. Indoors sensors were placed in strategic rooms of the building. Sensors for air temperature, air humidity, state of the doors and windows (open/closed), air-conditioners power consumption, water flow and water temperature (in the kitchen and in the gymnasium bathrooms) were installed. The layout of the school and the localization of the sensors are shown in Fig. 1. The state of the doors and windows are digital readings and are denoted as 'D' in this figure.

A computer composed by an AMD Athlon 2 GHz processor, with 512 MB of RAM and 80 GB of disk collects locally all the sensory information. The sampling rate for all variables is 1 min. Five data-loggers were used. Two of them (the nearest to the PC) communicate with it via RS-232; the others, located further apart, employ the TCP/IP Ethernet network available in the school. As the gymnasium is located in a different building, and the Ethernet network does not reach this building, communication of the water flow and temperature of the gymnasium bathrooms is performed by radio frequency.

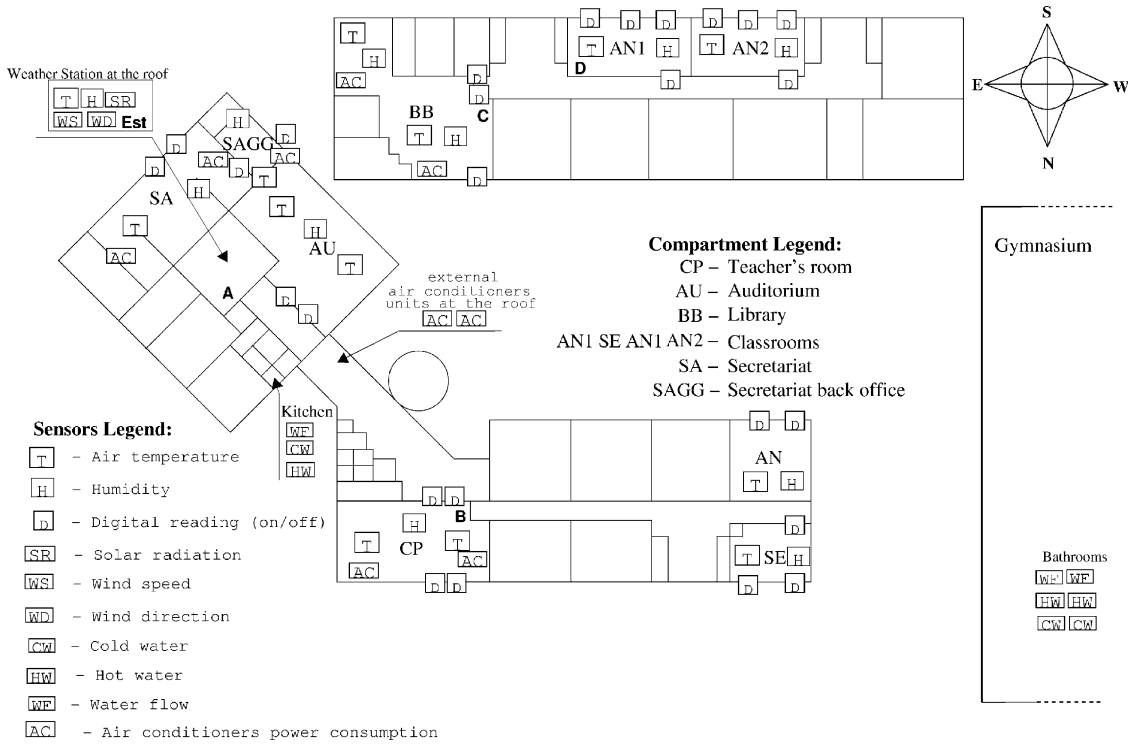

Fig. 1. School layout and sensor localization.

The data stored in the school PC is automatic transferred, hourly, via Internet, to a data server located in the Centre for Intelligent Systems, in the University of Algarve. This data server stores all the data and makes it available for the users via a WEB interface. This interface enables the user to select the relevant sensors, the time duration of the readings and the data format. A more detailed description of the remote data acquisition system can be found in Ref. [14].

3. Physical model

The multi-nodal building thermal behaviour physical model (please see further details in Refs. [15,16]) that works in transient conditions, is based in energy and mass balance integral equations. The energy balance integral equations are developed for the air inside the several compartments and ducts system, the different windows glasses, the interior bodies located inside the several spaces and the different slices of building main bodies and ducts system. The mass balance integral equations are developed for the water vapour (inside the several spaces, ducts system and in the interior surfaces of the windows glasses and interior and main bodies) and air contaminants (inside the several spaces and ducts system). For the resolution of this system of equations the Runge–Kutta–Fehlberg method with error control is used.

The physical model considers the conductive, convective, radiative and mass transfer phenomena. The conduction is verified in the building main bodies (door, ceiling, ground, wall, etc.) and ducts system (air or water transport) slices. In the convection the natural, forced and mixed phenomena are considered, while in the radiation, verified inside and outside the building, the short-wave (the real distribution of direct solar radiation in external and internal surfaces) and long-wave (heat exchange between the building external surfaces and the surrounding surfaces and heat exchange between the internal surfaces of each space) phenomena are taken into account. In the radiative calculus the shading effect caused by the surrounding surfaces and by the internal surfaces are also considered.

3.1. Input data

The model employs the building geometry, the construction materials and other conditions. In the three-dimensional geometry the compartments are defined through the introduction of involving bodies: building main bodies and windows glasses bodies. These bodies, with complex geometry, are associated to the boundary of two compartments or of a compartment and the external environment. As the main bodies are divided in several slices, in order to simulate the thermal stratification verified in these bodies, it is also necessary to identify the slices thickness. Inside each compartment it is important to introduce the more relevant interior bodies. The materials thermal proprieties are introduced for the main bodies, windows glasses and interior bodies. It is also necessary to introduce the external environmental and geographical conditions, the simulation initial conditions, the heat load released by the human bodies, heating and air-conditioning systems (and other internal sources), the occupation cycle, the occupants clothing and activity level, the air recirculation, the

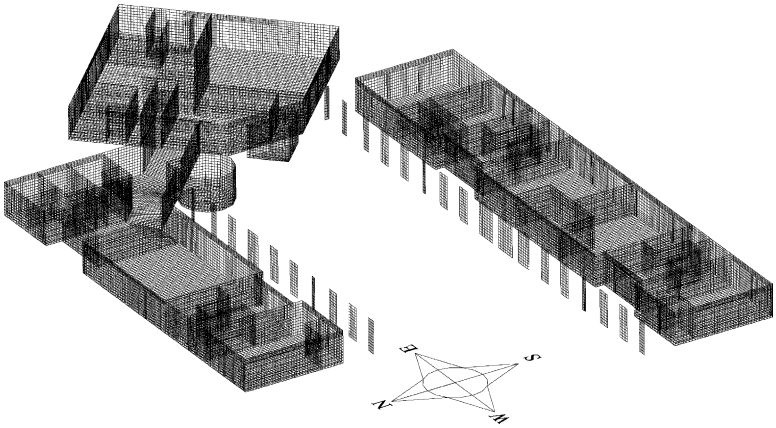

Fig. 2. Scheme of grid generation used by the physical model for the first floor.

air exchanges between compartments, the air exchange between each compartment and the external environment, and the internal mass generation and its intensity.

3.2. Grid generation

In the modern school building analyzed, with three floor levels, divided in 97 compartments, 1277 building main bodies and 211 window glasses were considered. In relation to the main bodies all existing external bodies that promote shading effect were also taken into account. The grid generation used the numerical simulation is presented in Fig. 2, for the first floor. This numerical grid, used in the internal and external direct solar radiation determination, was spaced 30 cm in both directions.

3.3. Winter validation and simulation

The validation and simulation is done in a typical Winter day (18 January 2004). During this study the sky was clear, the doors and windows were closed and the air-conditioning systems were off and the air mean renovation values inside each compartment by infiltration were obtained experimentally using the tracer gas concentration done in several compartments. The external environment inputs data were measured experimentally and the numerical model is built by 12,479 integral equations.

This simulation is divided in two parts. In the first one, used to validate the physical model, the air temperature numerical values are compared to the experimental values, while in the second one, after the numerical model validation, a real situation will be simulated. The occupation cycle, namely the teachers and students presence in the several spaces during all 18th January day will be taken into account. In this last situation a statistical study was performed, using different kinds of information, to evaluate the most realist occupations cycle in the different spaces of this school.

Results related with the air temperature evolution are presented in Fig. 3. In this figure the numerical values (with and without occupation) are depicted as continuous lines and the predicted data as points. In Fig. 3(a) the air temperature evolution in compartments with windows turned South is presented, in Fig. 3(b) with windows turned North, in Fig. 3(c) with windows turned Southeast and, finally, and in Fig. 3(d) with windows turned Southwest.

In conclusion, it was verified that the model reproduces well the experimental values. In general, the difference between numerical and experimental air temperature values is lower than 2 °C, a maximum difference of 4 °C was verified in the compartments with windows turned South, only during some hours in the afternoon. The lowest air temperature values were verified for compartments with windows turned North, while the highest values are verified for compartments with windows turned South.

In real situations, where the occupation cycle is considered, each compartment is characterized by an evolution of students and teachers during the day. Fig. 3 also shows the evolution of air temperature with occupation. In this statistical study lessons with 90 min and breaks with 15 min were assumed. In the compartments AN1 (see Fig. 3(a)) and SE (see Fig. 3(b)), used as classrooms, occupations of 24 students and 1 teacher (25 occupants) during the lessons (between 8:30 and 10:00 a.m., 10:15 and 11:45 a.m., 12:00 and 13:30 p.m., 13:45 and 15:15 p.m., 15:30 and 17:00 p.m., and 17:15 and 18:45 p.m.) and no occupation in the breaks were considered. In the compartment SA (see Fig. 3(c)), used as secretariat, 5 occupants between 8:30 a.m. and 18:45 p.m. were assumed, while for compartment AU (see Fig. 3(d)), used as an auditorium, an occupation of 90 persons during the lessons and none in the breaks was considered.

It was verified that the occupation cycle increases the air temperature level, the increase depending on the number of occupants. This value of the increasing of the air temperature is very important in the selection of the possible installation of heating system, during the Winter conditions, or air-conditioning system, in Summer conditions. Nevertheless, the option about the climatization system to be installed in the different compartments is associated not only with the air temperature values but also with the thermal comfort level, that also depends on the air velocity and relative humidity, the radiant

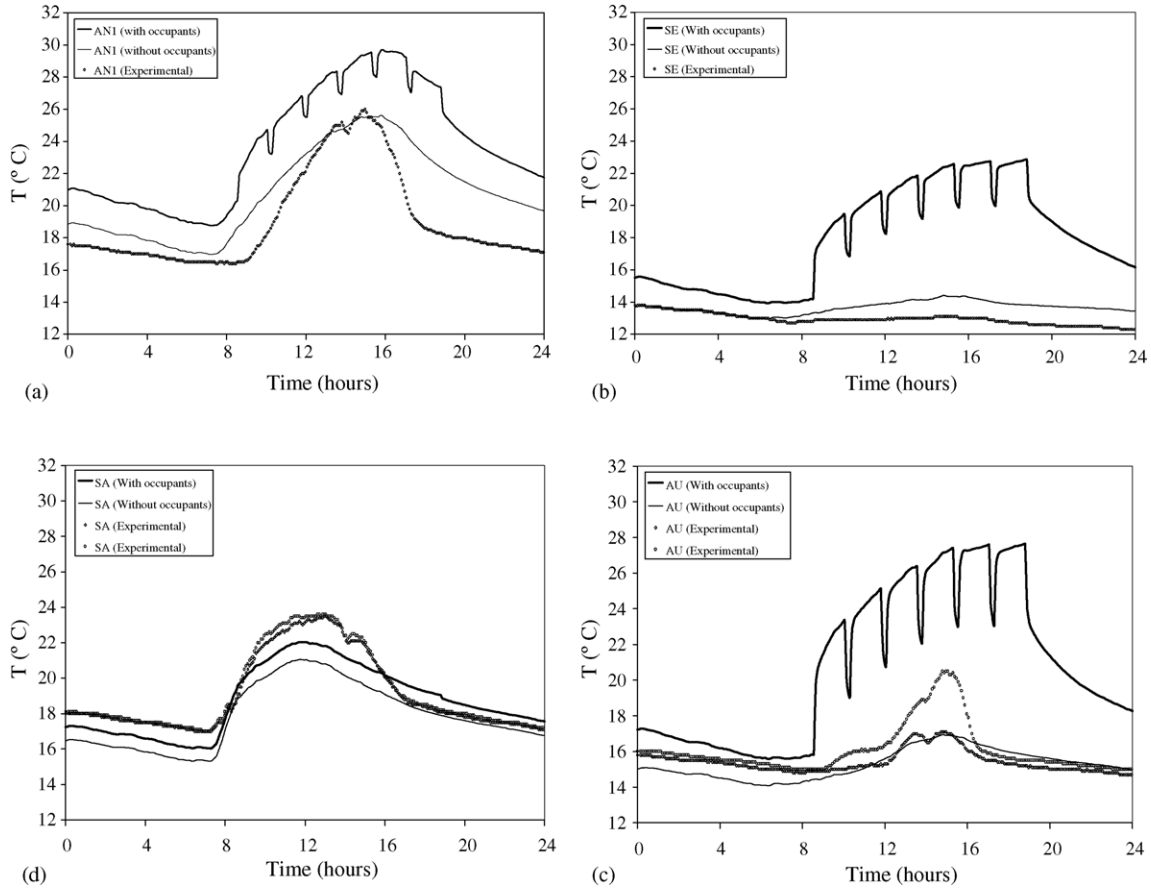

Fig. 3. Air temperature evolution in compartments with windows turned: (a) South, (b) North, (c) Southeast and (d) Southwest.

temperature and the clothing and activity levels. This topic will be analyzed in future works.

4. RBF neural network overview

Radial basis function (RBF) neural networks are composed of three functionally distinct layers. The input layer is simply a set of sensory units. The second layer is a hidden layer of sufficient dimension which performs a non-linear transformation of the input space to a hidden-unit space. The third and final layer performs a linear transformation from the hidden-unit space to the output space.

The topology of a RBF neural network is presented in Fig. 4. The output is given by:

$$\hat{y}(\boldsymbol{x}, \boldsymbol{w}, \boldsymbol{C}, \boldsymbol{\sigma}) = \sum_{i=1}^{n} w_i \varphi_i(\boldsymbol{x}, \boldsymbol{c}_i, \sigma_i) = \boldsymbol{\varphi}(\boldsymbol{x}, \boldsymbol{C}, \boldsymbol{\sigma})\boldsymbol{w}, \tag{1}$$

where n is the number of neurons, w_i the linear parameters, $\boldsymbol{c}_i$ the center vector and σ_i is the spread value for the ith neuron, and the non-linear function of the hidden neurons is:

$$\varphi_i(\boldsymbol{x}, \boldsymbol{c}_i, \sigma_i) = \mathrm{e}^{-||\boldsymbol{x}-\boldsymbol{c}_i||^2/2\sigma_i^2}, \quad \varphi_0 = 1, \tag{2}$$

where $||\ ||$ denotes the Euclidean norm.

For a specified number of neurons, and for a determined set of inputs (off-line), training a RBF network means to determine the value of $\boldsymbol{w}$, $\boldsymbol{c}_i$ and σ_i, such that (3) is minimized:

$$\Phi(\boldsymbol{X}, \boldsymbol{w}, \boldsymbol{C}, \boldsymbol{\sigma}) = \frac{||\boldsymbol{y}(\boldsymbol{X}) - \hat{\boldsymbol{y}}(\boldsymbol{X}, \boldsymbol{w}, \boldsymbol{C}, \boldsymbol{\sigma})||^2}{2}. \tag{3}$$

In the last equation, $\boldsymbol{y}$ denotes the actual output vector of the system which is being modelled, subject to the input data $\boldsymbol{X}$. Please note, that in contrast with (1) and (2), (3) is now applied to a set of input patterns, and not to a single input pattern.

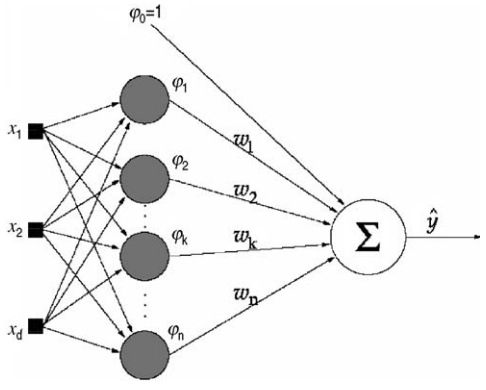

Fig. 4. A RBF network.

As the model output is a linear combination of the outputs of the hidden layer, (3) can be given as:

$$\Phi(\boldsymbol{X}, \boldsymbol{w}, \boldsymbol{C}, \boldsymbol{\sigma}) = \frac{||\boldsymbol{y}(\boldsymbol{X}) - \boldsymbol{\varphi}(\boldsymbol{X}, \boldsymbol{C}, \boldsymbol{\sigma})\boldsymbol{w}||^2}{2}. \quad (4)$$

Computing the global optimum value ($\boldsymbol{w}^*$) of the linear parameters $\boldsymbol{w}$ with respect to the non-linear parameters $\boldsymbol{C}$ and $\boldsymbol{\sigma}$ as a least-squares solution:

$$\boldsymbol{w}^* = \varphi^+(\boldsymbol{X}, \boldsymbol{C}, \boldsymbol{\sigma})\boldsymbol{y}(\boldsymbol{X}), \quad (5)$$

where "+" denotes a pseudo-inverse, and replacing (5) in (4), the training criterion to determine the non-linear parameters $\boldsymbol{C}$ and $\boldsymbol{\sigma}$ is:

$$\Psi(\boldsymbol{X}, \boldsymbol{C}, \boldsymbol{\sigma}) = \frac{||\boldsymbol{y}(\boldsymbol{X}) - \varphi(\boldsymbol{X}, \boldsymbol{C}, \boldsymbol{\sigma})\varphi^+(\boldsymbol{X}, \boldsymbol{C}, \boldsymbol{\sigma})\boldsymbol{y}(\boldsymbol{X})||^2}{2}, \quad (6)$$

which is now independent of the linear parameters $\boldsymbol{w}$. To minimize (6) the Levenberg–Marquardt method [17,18] is used. The hidden layer function centre positions are initialized by a clustering procedure known as the optimal adaptive k-means algorithm (OAKM) [19].

The initial spreads of the neuron activation functions are determined [20] using

$$\sigma_i = \frac{d_{\max}}{\sqrt{2\pi}}, \quad i = 1, \ldots, n, \quad (7)$$

where $d_{\max}$ is the maximum distance between the centers determined by the OAKM. The termination criterion used is the *early stopping* method that ends the training at the point of best performance in a test set. Further details concerning the training method can be found in Ref. [21].

5. Multi-objective genetic algorithm for structure determination and input selection

The procedure described in the preceding section for parameter estimation assumes that the network topology (number of neurons) is fixed and that the relevant inputs have been identified. Moreover, as the system to be modelled has dynamics, the number of input delayed terms and the actual lags for each input variable have to be determined.

The input variables considered in this phase of study are: inside air temperature (T_i), outside solar radiation (R_o), air temperature (T_o) and relative humidity (H_o). If T is the maximum number of model inputs, considering 4 input variables and 15 for the maximum lag for each variable, then $T = 4 \times 15 = 60$. If the number of model inputs is restricted to the interval [2, 30] and the number of neurons (n) to the interval [3, 10], the number of possible model combinations is in the order of 5 E18!

As it is not feasible to fully explore such a model space, a sub-optimal solution is obtained through the use of genetic algorithms. A genetic algorithm (GA) is an evolutionary computing approach in which a population-based search is performed by employing operators, such as selection, crossover and mutation. One of the advantages of GAs over other techniques is that they can be easily formulated as multi-objective optimizers providing a diverse set of solutions which meet a number of possibly conflicting objectives in a single run of the algorithm [22]. Each chromosome in the population represents a RBF model and is codified as a vector of integers, the first denoting the number of neurons, and the other integers entries to a matrix containing the admissible lagged terms for each input variable. For a detailed description of the application of multi-objective genetic algorithm to the design of radial basis function models please consult [23].

One MOGA run spans 100 generations. The population at each generation is composed of 100 RBF neural network candidate models. The objectives can be classified into three groups: model complexity, model performance and model validity. Regarding model complexity, the Euclidean norm of the RBF neural network linear weights ($||\boldsymbol{w}||$) and the number of non-linear parameters (NNLP) were employed. NNLP is calculated as follows:

$$\text{NNLP} = (n + 1)d, \quad (8)$$

where n is the number of centres and d is the number of model inputs. For the performance objectives the statistic indicator root mean square error (RMSE) and the maximum error (ME) on the training (tr), test (te) and validation (va) data sets were employed. Correlation-based validity tests [24] are used as model validation objectives. The following tests are used:

$$\begin{aligned}
&R_{ee}(\tau) = \delta(\tau) \\
&R_{ue}(\tau) = 0, \quad \forall\tau \\
&R_{u^2 e}(\tau) = 0, \quad \forall\tau \\
&R_{u^2 e^2}(\tau) = 0, \quad \forall\tau \\
&R_{e(eu)}(\tau) = 0, \quad \tau \geq 0 \\
&R_{e^2 e^2}(\tau) = \delta(\tau) \\
&R_{(ye)e^2}(\tau) = k\delta(\tau) \\
&R_{(ye)u^2}(\tau) = 0, \quad \forall\tau
\end{aligned} \quad (9)$$

If the normalized correlation functions (9) lie within the 95% confidence bands at $1.96/\sqrt{N}$, N being the size of the data vectors, the model is considered adequate.

During the MOGA optimization each individual in the population is trained, with the data belonging to the training set, for one-step-ahead prediction using the Levenberg–Marquardt method presented in the last section. The training is terminated using the early stopping criteria in the test set. The RBF neural network trained with this procedure is subsequently evaluated in the validation set.

Different models were designed for several rooms of the building, where sensors were located. In this example the room denoted as AN1 in Fig. 1 is used. All the data taken were acquired during no activity, that is, without people or equipment that could change the inside environment.

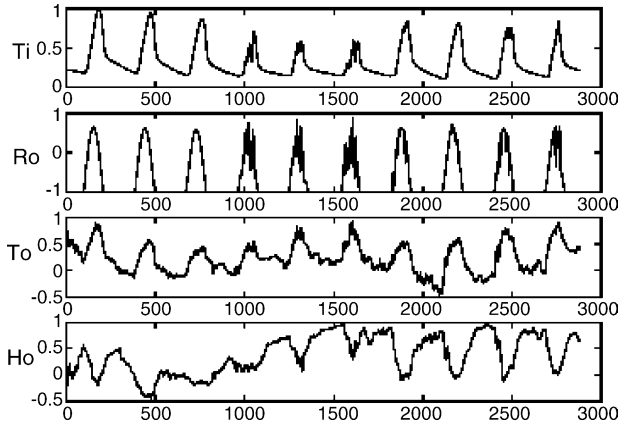

Fig. 5. Normalized training data.

The data set is composed of:

training set—10 days (22–31 December 2003), 2880 points;
test set—3 days (2–4 January 2004), 864 points;
validation set—1 day (4 January 2004), 288 points;
comparison set—1 day (18 January 2004), 288 points.

The aim of the comparison set is to compare the results obtained with the neural model with the ones obtained with the physical model. The sampling rate used was 5 min, which means that five samples acquired with 1 min sampling rate are averaged, before training is performed. The data set is afterwards pre-processed, scaling the data between [−1, 1]. Fig. 5 shows the normalized training data set.

The MOGA parameters employed are shown in Table 1.

The use of the complexity objectives were considered as the most important ones in order not to obtain badly conditioned models and complex networks. The complexity goals used are sufficiently large to give some freedom to the MOGA optimization process. Four MOGA runs were processed. The results of each run were analyzed and the goals for the subsequent goals were adjusted. The final goals and priorities are also shown in Table 1.

According to the goals and preferences set, five models were obtained in the preferable set. The results are summarized in Tables 2–4.

Table 2
Input lags

	T_i	R_o	T_o	H_o
N_1	1–4, 6, 8–10, 14	6, 8, 11, 14, 15	3, 4, 7	–
N_2	1, 2, 7, 9, 10, 13, 15	8, 12, 13, 15	12, 14	11
N_3	1–3, 5, 9, 10, 15	11–13, 15	10, 14, 15	11
N_4	1, 2, 4, 5, 9, 10, 13, 15	11–15	10, 12–14	11
N_5	1–4, 6–8, 14, 15	8, 11–15	3, 5, 7, 12, 15	–

From Table 2 is possible to verify that the model structure in the preferable set is highly based in the inside temperature inputs.

All the goals related with performance and complexities were met (underlined in Table 3), except the one related with the maximum error in the training set.

The correlation tests for validation (Table 4) did not achieve the proposed goals due to the great non-linearity of the problem. The NN selected from the preferable set was N1, as it was the one who achieved the minimum value (underlined in the table) in five out of the eight tests.

Fig. 6 shows the outputs of the N1 model and the physical model in the comparison set. The RMSE for the neural network and the physical model were 0.0493 and 0.1777, respectively, which means that the RBF model is 3.5 better than the physical model. The error distribution (Fig. 7) shows that the RBF network model generates error centred in 0, while in the physical model a bias is evident. It should be pointed out that, to perform a fair comparison between the models, the RBF model used, as lagged inputs for the internal temperature, values fed back from the model output and not from the measured temperature, as employed for training. This is also the reason why outside relative air humidity was employed and not inside relative air humidity.

The model presented so far was designed with data belonging to periods where no activity was present. At a second stage, the same room (a classroom) was considered, but with data belonging to periods where the building was occupied, and where the door and windows were open and closed. Specifically data between 1 and 5 March 2004 and between 8 and 12 March 2004 were used as training data,

Table 1
MOGA parameters and objectives

MOGA parameters		MOGA objectives					
		Objective	Goal	Priority	Objective	Goal	Priority
Chromosome length	31	$RMSE_{tr}$	0.006	2	R_{ee}	0.036	1
Number of individuals	100	$RMSE_{te}$	0.004	2	$R_{e^2e^2}$	0.036	1
Number of generations	100	$RMSE_{va}$	0.035	2	$R_{(ye)e^2}$	0.036	1
Proportion of random immigrants (%)	10	ME_{tr}	0.07	1	$R_{(ye)u^2}$	0.036	1
Selective pressure	2	ME_{te}	0.03	1	R_{ue}	0.036	1
Crossover rate	0.7	ME_{va}	0.1	1	$R_{u^2'e^2}$	0.036	1
Survival rate	0.5	$\|\|\boldsymbol{w}\|\|$	50	3	$R_{u^2'e}$	0.036	1
Number of neurons interval	[3, 10]	NNLP	500	3	$R_{e(eu)}$	0.036	1
Maximum number of inputs	30						
Maximum lag	15						

Table 3
Performance and complexity results

	$RMSE_{tr}$	$RMSE_{te}$	$RMSE_{va}$	ME_{tr}	ME_{te}	ME_{va}	$\|\|w\|\|$	NNLP	d
N_1	0.006	0.004	0.034	0.075	0.026	0.072	4.66	144	17
N_2	0.006	0.004	0.032	0.071	0.024	0.085	8.44	135	14
N_3	0.006	0.004	0.034	0.075	0.021	0.083	5.32	128	15
N_4	0.006	0.004	0.030	0.073	0.022	0.070	6.21	171	18
N_5	0.006	0.004	0.033	0.071	0.028	0.110	6.23	126	20

Table 4
Validity tests

	R_{ee}	$R_{e^2e^2}$	$R_{(ye)e^2}$	$R_{(ye)u^2}$	R_{ue}	$R_{u^2{}'e^2}$	$R_{u^2{}'e}$	$R_{e(eu)}$
N_1	0.060	0.239	0.107	0.070	0.113	0.314	0.072	0.068
N_2	0.088	0.258	0.133	0.067	0.105	0.314	0.076	0.120
N_3	0.083	0.239	0.138	0.084	0.117	0.310	0.085	0.093
N_4	0.075	0.243	0.130	0.084	0.114	0.311	0.089	0.091
N_5	0.113	0.269	0.140	0.079	0.122	0.329	0.081	0.120

between 15 and 20 March 2004 as test data, and between 23 and 28 March 2004 as validation data. Inside air relative humidity was used instead of outside relative air humidity. The following variables were added to the set of input variables: door state, D (open—1/closed—0); windows state, W [0–3] (0 being all windows closed and 3 all the three windows open), wind direction and velocity.

A similar design procedure was conducted for this data with the objectives shown in Table 5.

The chosen model (out of 10 models in the preferential set) had the input vector presented in Table 6. Please note that the sampling time used here was 15 min, as experiments conducted with 5, 10 and 15 min presented similar results. As it can be seen, the wind components were not considered as relevant by multi-objective genetic algorithm.

Tables 7 and 8 presents the results obtained by the chosen model.

As expected, the results obtained for the period where the building is fully functioning are slightly worse than in the previous case, where all windows and doors were closed and the building was not occupied. Still the results obtained are very satisfactory.

6. Adaptive model

Neural networks are non-linear models which need, for a satisfactory performance, that the data used for the training process covers all the range of its inputs and outputs, and that there is a uniform coverage of data within this range. For the case at hand, as the models described before were trained with data belonging to the Winter and to the Spring period, a satisfactory performance of these models, say, in Summer should not be expected.

To illustrate this, the model developed with data from March was executed with data from April to August. The results are presented in Fig. 8.

As it can be seen the error is small in April (where the weather data does not differ significantly from the data used for

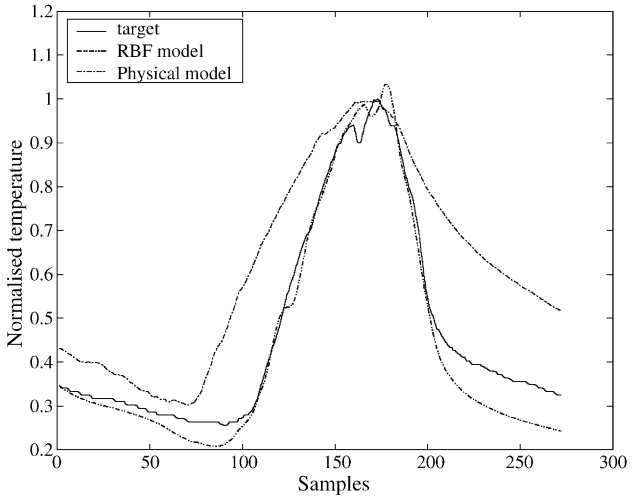

Fig. 6. Model outputs and target for the comparison set.

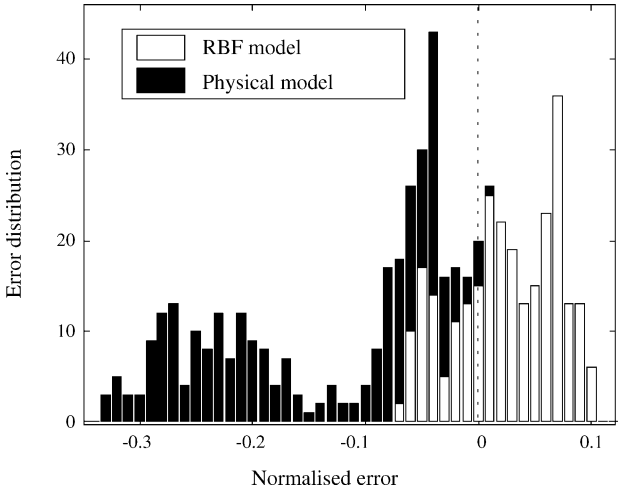

Fig. 7. Error distribution.

Table 5
MOGA objectives

Objective	$RMSE_{tr}$	$RMSE_{te}$	ME_{te}	$\|\|\boldsymbol{w}\|\|$	NNLP	R_{ee}	$R_{e^2e^2}$	$R_{(ye)e^2}$
Goal	0.02	0.02	0.15	50	500	0.07	0.07	0.07
Priority	2	2	1	1	1	1	1	1

Objective	$R_{(ye)e^2}$	$R_{(ye)u^2}$	R_{ue}	$R_{u^2'e^2}$	$R_{u^2'e}$	$R_{e(eu)}$
Goal	0.07	0.07	0.07	0.07	0.07	0.07
Priority	1	1	1	1	1	1

training, March) and deteriorates when the summer period arrives.

However, one of the big advantages of neural networks is that they can be made adaptive, by changing their parameters according to the current performance. There are two main classes of adaptive algorithms: ones that just adapt the linear parameters, keeping the non-linear structure fixed, and others that adapt all the network parameters. Here the latter approach is followed. In terms of the amount of data used for computing the update, the algorithms can also be classified into those that perform this update with just the current data sample, and those that use for that a sliding window. The former are essentially recursive implementations of off-line algorithms while in the latter case the off-line algorithms can be employed directly, with minor modifications. The approach followed here is the latter, the use of the off-line training method described in Section 4, to a sliding window of data.

The following modifications were introduced to the off-line algorithm:

The data used for training, in instant k, are stored in a sliding window which is also updated in each instant, using a FIFO policy—the current pair input-target data replaces the oldest pair stored in the window.

The initial values of the network parameters, for instant k, are the final values of the optimization conducted in instant $k-1$. The initial value of the regularization parameter of the Levenberg–Marquardt method is the final value of the last optimization. This is justified as abrupt changes, from instant to instant, are not expected. In the first instant the network parameters are initialized with values obtained from an off-line training procedure and the regularization parameter is initialized to 1. In this example the model determined with data from March was used as the initial model.

As there is no test set to terminate the optimization, the early stopping method cannot be employed. Instead, a set of termination criteria, which must be simultaneously satisfied, is used. In (10) τ_f denotes the user-defined precision, in terms of significant digits in the training criterion, $\boldsymbol{v}$ is the vector of the non-linear parameters (in this case the centers and the spreads) and $\boldsymbol{g}$ is the gradient vector for criterion Ψ. Here, a value of 0.01 was used for τ_f.

$$\begin{aligned} &\Psi_{k-1} - \Psi_k < \tau_f(1 + \Psi_k) \\ &||\boldsymbol{v}_{k-1} - \boldsymbol{v}_k|| < \sqrt{\tau_f}(1 + ||\boldsymbol{v}_k||) \\ &||\boldsymbol{g}_k|| \leq \sqrt[3]{\tau_f}(1 + \Psi_k) \end{aligned} \tag{10}$$

A common problem found in adaptive models is that, in many cases, the adapted model ''forgets'' what it has learned previously and becomes tuned to just the most recent data. This phenomenon is related with the size of the sliding window. An experiment was conducted, experimenting three different window sizes: 1 day of data, 3 days and 8 days. The data employed covered the months of April–August 2004. Table 9 summarizes the results.

In Table 9, T_a denotes the RMSE obtained for all data with the on-line adaptive model, T_f the RMSE obtained for all data with the fixed model obtained in the last instant, $\bar{N}_i$ the average number of the optimization iterations and $\bar{C}_t$ is the average

Table 6
Input lags

T_i	1, 2, 10, 16, 17
R_o	1, 2, 4, 6–8, 10
T_o	11, 12, 16
H_i	8, 9
W	1, 2, 6, 8, 14, 19, 21
D	1, 2

Table 7
Performance and complexity results

$RMSE_{tr}$	0.02
$RMSE_{te}$	0.02
$RMSE_{va}$	0.03
ME_{te}	0.11
ME_{va}	0.14
$\|\|\boldsymbol{w}\|\|$	13.8
NNLP	81
d	26
n	3

Table 8
Validity tests

R_{ee}	0.056
$R_{e^2e^2}$	0.043
$R_{(ye)e^2}$	0.074
$R_{(ye)u^2}$	0.132
R_{ue}	0.081
$R_{u^2'e^2}$	0.421
$R_{u^2'e}$	0.113
$R_{e(eu)}$	0.076

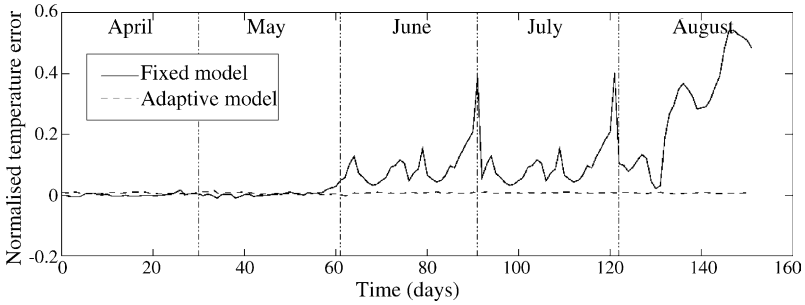

Fig. 8. Evolution of the error. Adaptive model vs. fixed model.

computational time, per instant. As it can be seen by analyzing T_a, all three window sizes achieve a similar result using on-line adaptation, but the model obtained using a window size of 8 days achieves a value for T_f very similar to T_a, and one order of magnitude smaller than with a window size of 1 day. This indicates that the ''forgetting problem'' is much more severe with smaller window sizes. On average, the adaptation algorithm just computes one iteration per sampling instant in all cases considered. The average computing time, per sampling instant, using a 1333 MHz Athlon AMD PC, is just around 43 ms for an 8 days window.

Using a window size of 8 days, the evolution of the error in the 5 months under study is shown in Fig. 8. Comparing with the fixed model it is clear that with this adaptive scheme, a very good constant performance can be obtained, throughout the year. The RMSE for the fixed model is 0.208, while for the adaptive model is 0.013.

To enable a more detailed inspection of the results, Fig. 9 shows the predicted and measured temperature, for a typical week in 25–30 of May, for the fixed model and the adaptive model.

7. Control of an air-conditioned system

Finally, the use of predictive models for the control of an air-conditioned system is illustrated using a very simple simulation. The chosen room was the school library, identified as BB in Fig. 1, which has two air-conditioned systems. As it is the case in the majority of secondary school buildings in Portugal, only a few rooms have air-conditioned systems, which are manually controlled via the device remote control. The remote data acquisition system described in Section 2 only monitored the power consumption of the air conditioners (which enables to detect the on/off state of the systems), and there was no control or record of the reference temperature set by the users. As there was not the possibility of automatically controlling the air-conditioned systems at this time, the aim of this simulation example is to shown that even with a very simple and naïve anticipative on/off control strategy, energy savings and better temperature regulation could be achieved with long-range predictive models.

Table 9
Results with different window sizes

Window size (days)	T_a	T_f	$\bar{N}_i$	$\bar{C}_t$ (ms)
1	0.014	0.193	1.0001	8.3
3	0.012	0.059	1.0001	16.5
8	0.013	0.018	1.0069	42.9

As the air temperature depends in this case also on the air conditioners state and their reference temperature, these variables should also be used as inputs to the neural model. Therefore, the state $-AC_i-$ (0—off, 1—on) and the reference temperature (RT_i) of each device were considered as input variables. As the reference temperature is not measured, it was indirectly inferred as the steady state temperature of the room, when the air conditioners were working. Additional input variables considered were the inside air temperature (T_i) and relative humidity (H_i), and the outside solar radiation (R_o) and air temperature (T_o). The variable that will be estimated is the room air temperature which, in this case, is the average of the readings of the two air temperature sensors located in the room.

The model is to be used not for 1-step-ahead prediction, as in the previous cases, but for long-range prediction (an horizon h of 96 steps ahead in the future was considered, with a sampling time of 5 min).

Fig. 10 illustrates that this long-range prediction is achieved as a sequence of a sequence of one-step-ahead predictions. At instant k, the delayed values of the inside air temperature used as inputs to the neural model are whether past measured values or estimated values, if the time stamp related with the particular input is less or equal k, or greater than k, respectively. If this approach would be used in practice, the same reasoning should apply to the outside solar radiation and air temperature, and to the inside air relative humidity, which is also dependent on the inside air temperature.

Neural networks can be designed with multi-objective generic algorithm for this purpose (please see Ref. [25] for details), but for the purpose of this simple example measured data was used.

The data set used in this example is composed of:

training data—1 to 7 June 2004;
test data—8 to 14 June 2004;
validation data—14–21 June 2004.

The training data was used, as before, by the Levenberg–Marquardt algorithm to estimate the model parameters, and the test data for early stopping. The priority of the performance objectives used for MOGA was related with the intended use

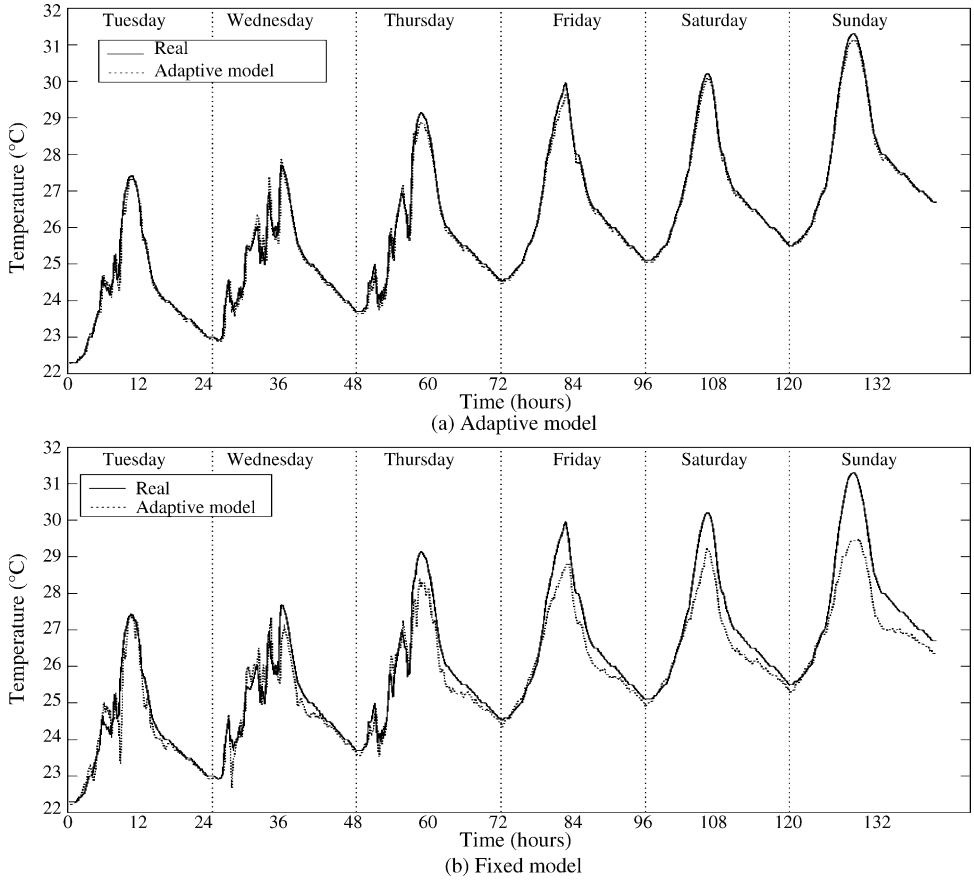

Fig. 9. Adaptive model vs. fixed model.

of the model. Two high-priority objectives were employed: $MRMSE_p$, which is the maximum of the RMSEs obtained for each prediction horizon, over the training and test samples, and $MRMSE_k$, which is the maximum of the RMSEs obtained for each step-ahead prediction, over the training and test samples.

The MOGA objectives were set as expressed in Table 10. A value of infinity in the goal and a priority of 0 means that the objective is simply optimized, and not treated as a restriction to be met.

The inputs of the chosen model and the results are presented in Table 11. Tables 12 and 13 present the results obtained by the chosen model.

This model was subsequently used for a very simple anticipative on/off control. The library working hours were from 8 to 16 h. It was assumed that the inside air temperature,

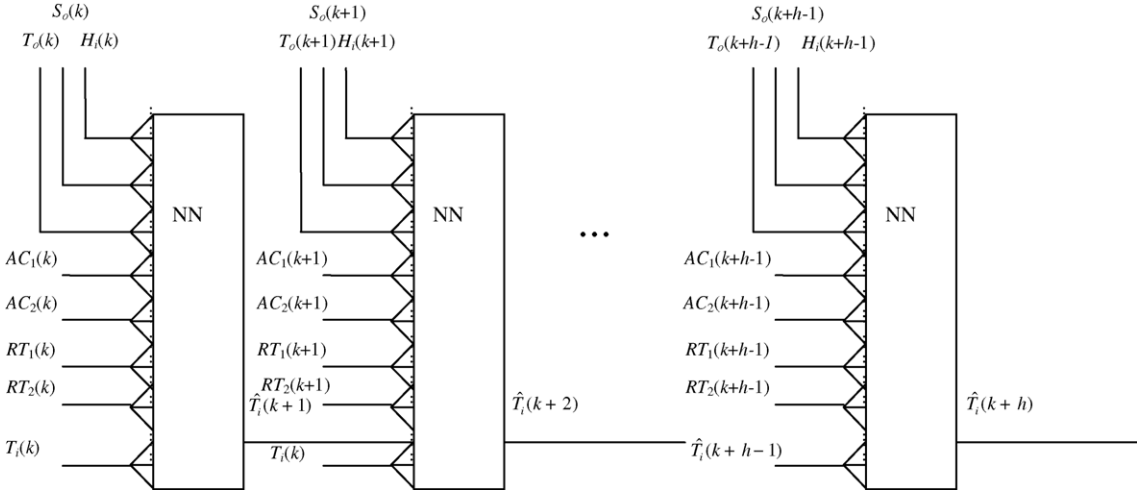

Fig. 10. Long-range air temperature prediction.

Table 10
MOGA objectives

Objective	$RMSE_{tr}$	$RMSE_{te}$	$MRMSE_p$	$MRMSE_k$	ME_{tr}	ME_{te}	$\|\|w\|\|$	NNLP
Goal	Infinity	Infinity	0.01	0.01	Infinity	Infinity	30	500
Priority	0	0	2	2	0	0	3	3

Objective	R_{ee}	$R_{e^2e^2}$	$R_{(ye)e^2}$	$R_{(ye)u^2}$	R_{ue}	$R_{u^2'e^2}$	$R_{u^2'e}$	$R_{e(eu)}$
Goal	0.039	0.039	0.039	0.039	0.039	0.039	0.039	0.039
Priority	1	1	1	1	1	1	1	1

Table 11
Input lags

T_i	6
R_o	1, 2, 5, 6, 9, 10
T_o	1, 3, 8, 11, 14
H_i	5, 10, 13, 14
AC_1	5
AC_2	5
RT_1	1
RT_2	2–5

Table 12
Performance and complexity results

$RMSE_{tr}$	0.0077
$RMSE_{te}$	0.0110
$MRMSE_p$	0.0248
$MRMSE_k$	0.0300
ME_{tr}	0.0573
ME_{te}	0.0654
$\|\|w\|\|$	4.8
NNLP	240
d	23
n	10

during the working period for each day, should be regulated within an interval of +1 and −0.7 °C around the average measured temperature for that particular day. In order to do that, in each sampling instant the air temperature is forecasted 30 min in the future. If within this prediction horizon it is forecasted that the temperature exceeds the high limit, then the two air-conditioned systems are turned on. If, on the other hand, it is predicted that the temperature will be less than the low limit, then the two systems are turned off. This very simple strategy was chosen just to validate the predictive model and should not be envisaged as a control methodology, which should be predictive control.

Table 13
Validity tests

R_{ee}	0.8811
$R_{e^2e^2}$	0.7538
$R_{(ye)e^2}$	0.0609
$R_{(ye)u^2}$	0.1994
R_{ue}	0.1919
$R_{u^2'e^2}$	0.3912
$R_{u^2'e}$	0.1963
$R_{e(eu)}$	0.8765

Figs. 11 and 12 show simulations of this control strategy for the days 15 and 24 June. The real periods of the manual operation of the air conditioners are marked in the figures, as well as the measured temperature.

As it can be seen, the temperature is regulated within the specified limits, and with important savings in energy. Extending this simulation through all the working days of

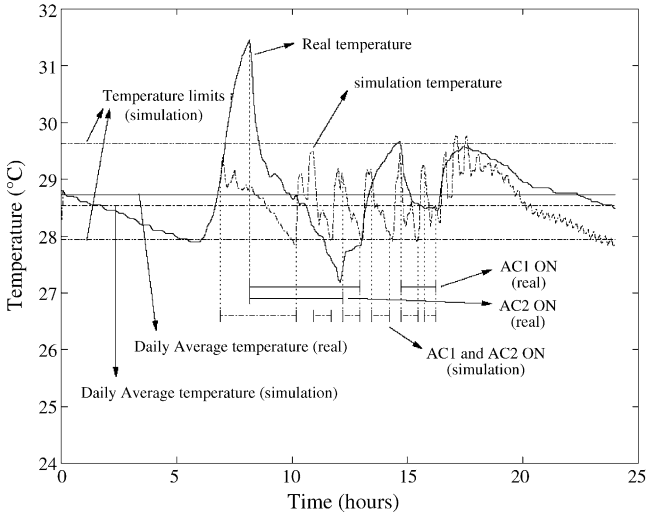

Fig. 11. Simulation for 15 June.

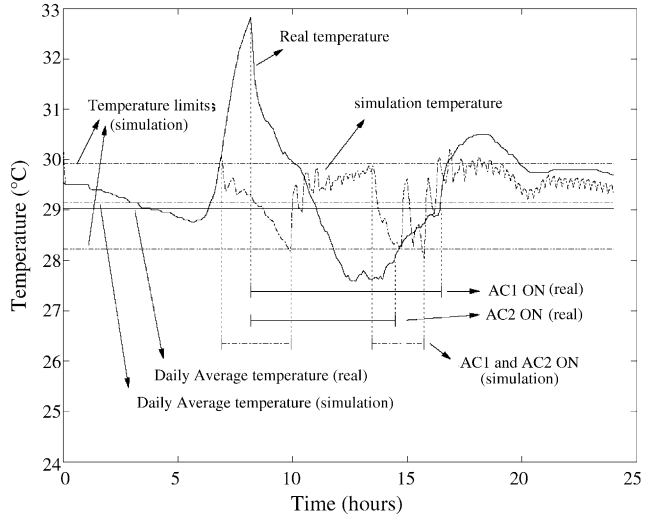

Fig. 12. Simulation for 24 June.

June, using this simple methodology, a 27% reduction of the use of the air conditioners was verified, with the temperature staying within the specified limits, for the whole working period (which obviously does not happen with manual control).

8. Conclusions and future work

In this paper the use of neural networks for air temperature prediction inside buildings was discussed. It was shown that by using multi-objective genetic algorithms for the off-line design of radial basis function neural networks, the neural models can achieve better results than state-of-the-art physical models. By using a sliding window adaptive methodology, the good results obtained off-line can be extended throughout the whole year. The use of long-range predictive models for air-conditioning systems control has been demonstrated, in simulations, achieving a good temperature regulation with important energy savings.

Future work will address the control aspect. First, multi-objective genetic algorithm will be used for designing long-range prediction models of the outside solar energy and air temperature, in the lines of Ref. [25]. Then the commercial remote controllers will be replaced by computer-controlled remote controllers, so that the air-conditioning systems can be computer-controlled. With this scheme, richer data can be acquired for improving the long-range inside air temperature model, designed together with the long-range inside relative air humidity model (please see Ref. [25]). Finally, these models, adapted on-line as described in this paper, will be used in a predictive control strategy, weighting temperature regulation with energy spending, applied during the building working periods.

Acknowledgment

The authors wish to acknowledge the support of Feder and Inovalgarve 02–03 project.

References

[1] S. Kalogirou, Artificial neural networks in renewable energy systems applications: a review, Renewable & Sustainable Energy Reviews 5 (2001) 373–401.
[2] C. Cetiner, F. Halici, H. Cacur, et al., Generating hot water by solar energy and application of neural network, Applied Thermal Engineering 25 (2005) 8–9.
[3] A. Argiriou, I. Bellas-Velidis, C. Balaras, Development of a neural network heating controller for solar buildings, Neural Networks 13 (2000) 811–820.
[4] A. Ben-Nakhi, M. Mahmoud, Energy conservation in buildings through efficient A/C control using neural networks, Applied Energy 73 (2002) 5–23.
[5] S. Wang, Y. Chen, Fault-tolerant control for outdoor ventilation air flow rate in buildings based on neural network, Building and Environment 37 (2002) 691–794.
[6] M. Mahmoud, A. Ben-Nakhi, Architecture and performance of neural networks for efficient A/C control in buildings, Energy Conversion and Management 44 (2003) 3207–3226.
[7] A. Argiriou, I. Bellas-Velidis, M. Kummert, P. André, A neural network controller for hydronic heating systems of solar buildings, Neural Networks 17 (2004) 427–440.
[8] I. Yang, K. Kim, Prediction of the time of room air temperature descending for heating systems in buildings, Building and Environment 39 (2004) 19–29.
[9] A. Ben-Nakhi, M. Mahmoud, Cooling load prediction for buildings using general regression neural networks, Energy Conversion & Management 45 (2004) 2127–2141.
[10] G. Mikhlakakou, M. Santamouris, A. Tsangrassoulis, On the energy consumption in residential buildings, Energy and Buildings 34 (2002) 727–736.
[11] K. Funahashi, On the approximate realization of continuous mappings by neural networks, Neural Networks 2 (1989) 183–192.
[12] K. Hornik, M. Stinchcombe, H. White, Multilayer feedforward networks are universal approximators, Neural Networks 2 (1989) 359–366.
[13] F. Girosi, T. Poggio, Networks and the Best Approximation Property, Biological Cybernetics 63 (1990) 169–176.
[14] E.M. Crispim, M.D. Martins, A.E. Ruano, C.M. Fonseca, Remote data acquisition system of environmental data, in: Proceedings of the Sixth Portuguese Conference of Automatic Control (Controlo 2004), University of Algarve, June, 2004.
[15] E.Z.E. Conceição, Numerical simulation of buildings thermal behaviour and human thermal, comfort multi-node models, in: Proceedings of Building Simulation 2003—Eighth International IBPSA Conference, Eindhoven, Netherlands, 11–14 August, 2003.
[16] E.Z.E. Conceição, A.I. Silva, M.M.J.R. Lúcio, Numerical study of thermal response of school buildings in winter conditions, in: RoomVent'2004—Ninth International Conference on Air Distribution in Rooms, Portugal, Coimbra, 5–8 September, 2004.
[17] K. Levenberg, A method for the solution of certain problems in least squares, Quarterly Applied Mathematics 2 (1944) 164–168.
[18] D. Marquardt, An algorithm for least-squares estimation of nonlinear parameters, SIAM Journal of Applied Mathematics 11 (1963) 431–441.
[19] C. Chinrungrueng, C. Séquin, Optimal adaptive *k*-means algorithm with dynamic adjustment of learning rate, IEEE Transactions on Neural Networks 1 (6) (1995) 157–169.
[20] S. Haykin, Learning strategies, in: Neural Networks: A Comprehensive Foundation, second ed., Prentice Hall, 1998.
[21] P.M. Ferreira, E.A. Faria, A.E. Ruano, Neural network models in greenhouse air temperature prediction, Neurocomputing 1 (43) (2002) 51–75.
[22] C.M. Fonseca, P.J. Fleming, Multiobjective optimization and multiple constraint handling with evolutionary algorithms: a unified formulation, IEEE Transactions on Systems, Man and Cybernetics—Part A: System and Humans 1 (28) (1998) 26–37.
[23] P.M. Ferreira, A.E. Ruano, C.M. Fonseca, Genetic assisted selection of model structures for greenhouse inside air temperature prediction, in: Proceedings of the 2003 IEEE Conference on Control Applications (CCA 2003), 2003, pp. 576–581.
[24] S. Billings, Q. Zhu, Nonlinear Model Validation using Correlation Tests, Department of Automatic Control and Systems Engineering, University of Sheffield, Sheffield S14DU, UK, 1993 (Research Report 463).
[25] P.M. Ferreira, A.E. Ruano, C.M. Fonseca, Evolutionary multiobjective design of radial basis function networks for greenhouse environmental control, in: 16th IFAC World Congress, Prague, July, 2005.